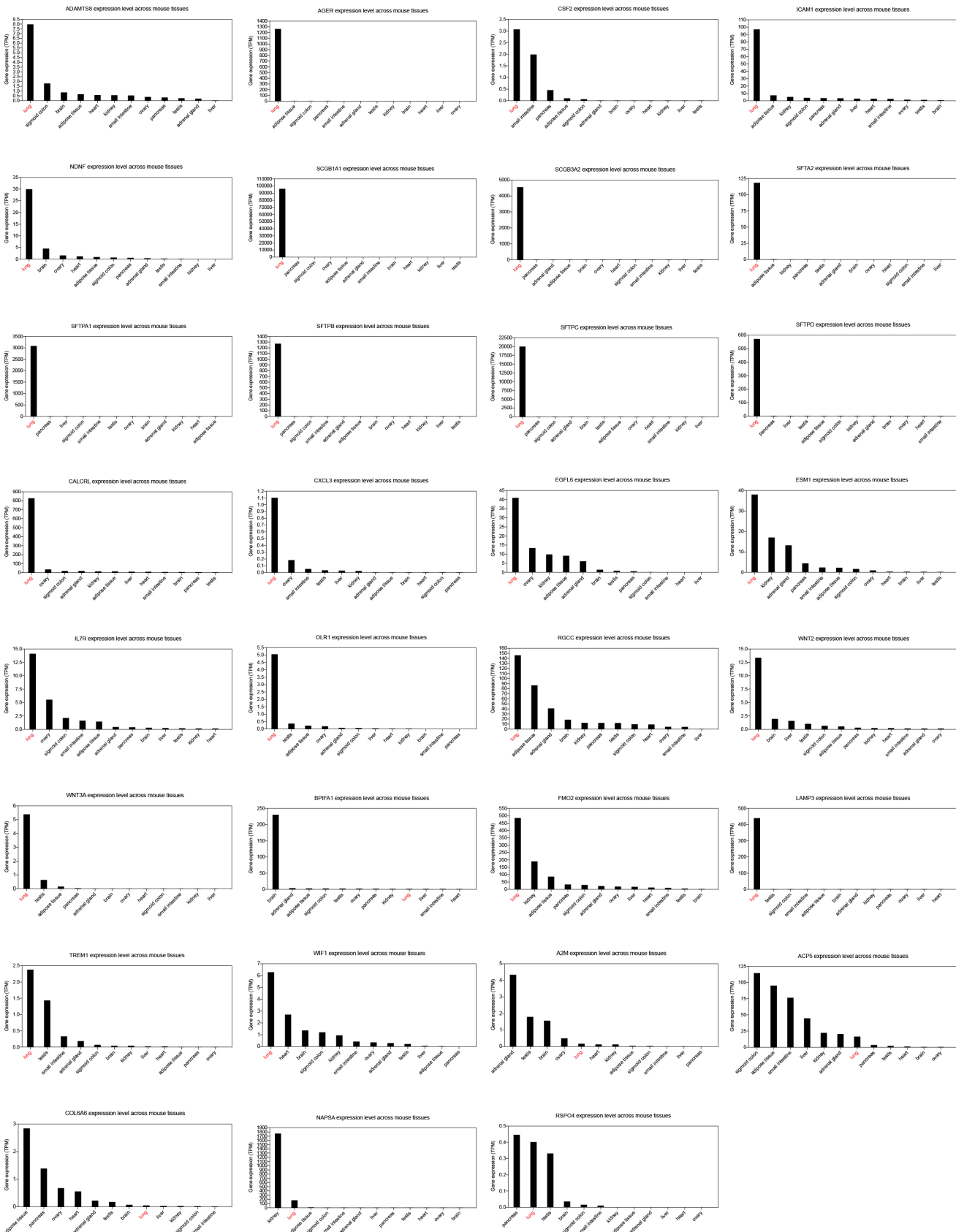


**Supplementary Figure 1. mRNA expression of the top-ranking sLungGenes in 37 normal adult human tissues from the HPA database**

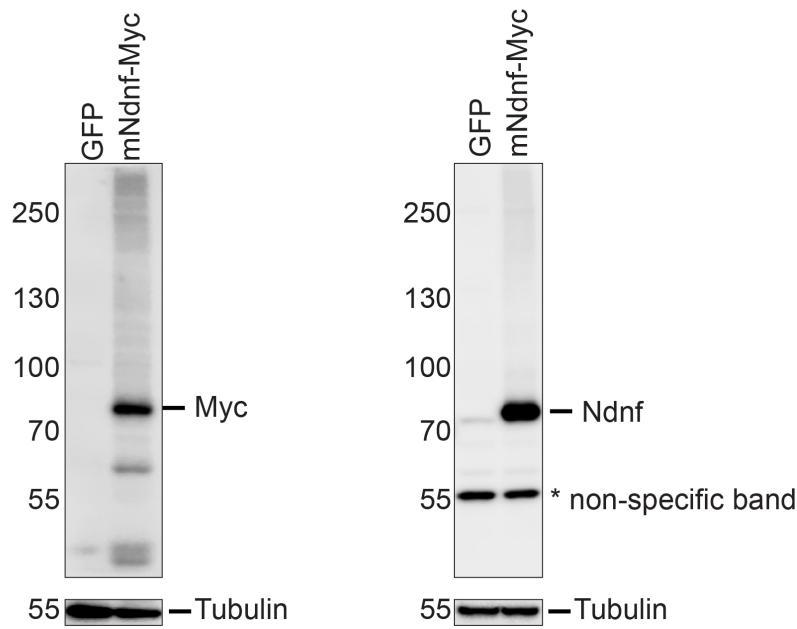
Transcript abundance for each of the identified top-ranking sLungGenes were downloaded from the HPA database and plotted across 37 normal adult human tissues.





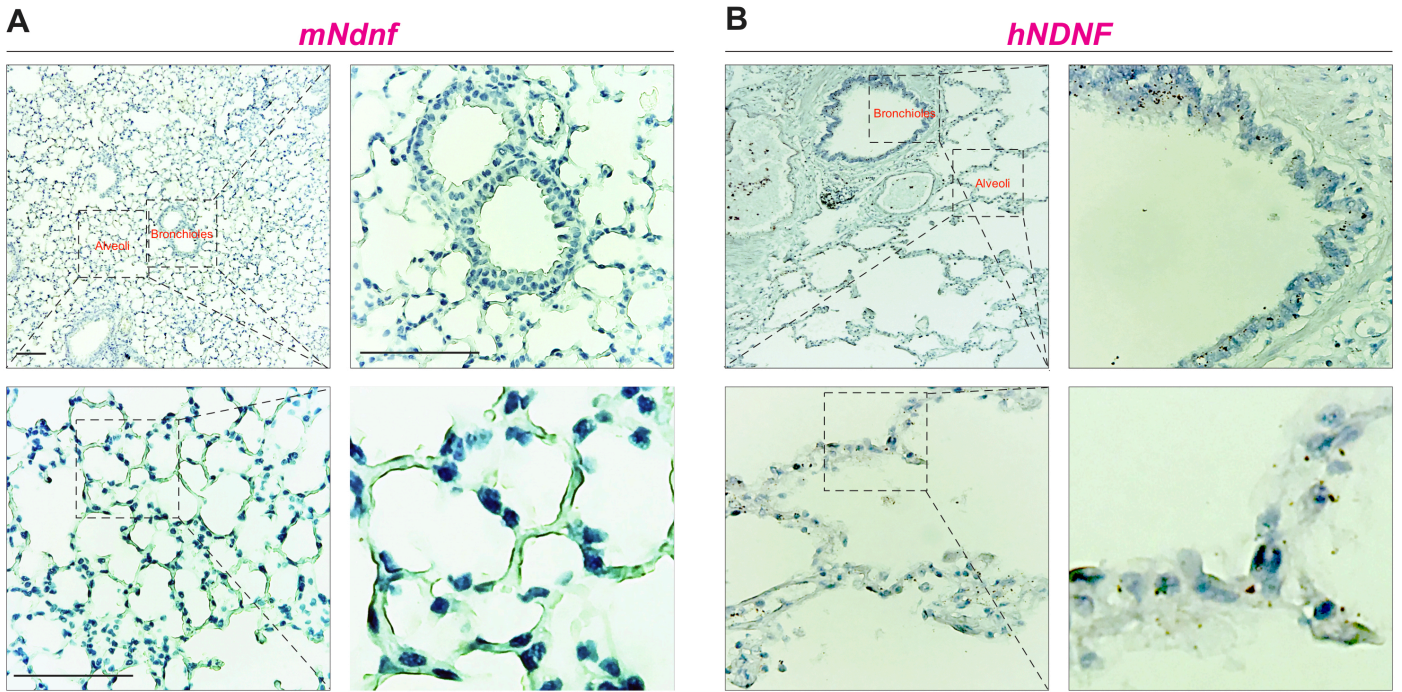
### Supplementary Figure 3. mRNA expression of the top-ranking sLungGenes in 12 normal adult mouse tissues from the ENCODE database

Transcript abundance for each of the identified top-ranking sLungGenes were downloaded from the ENCODE database and plotted across 12 normal adult mouse tissues.



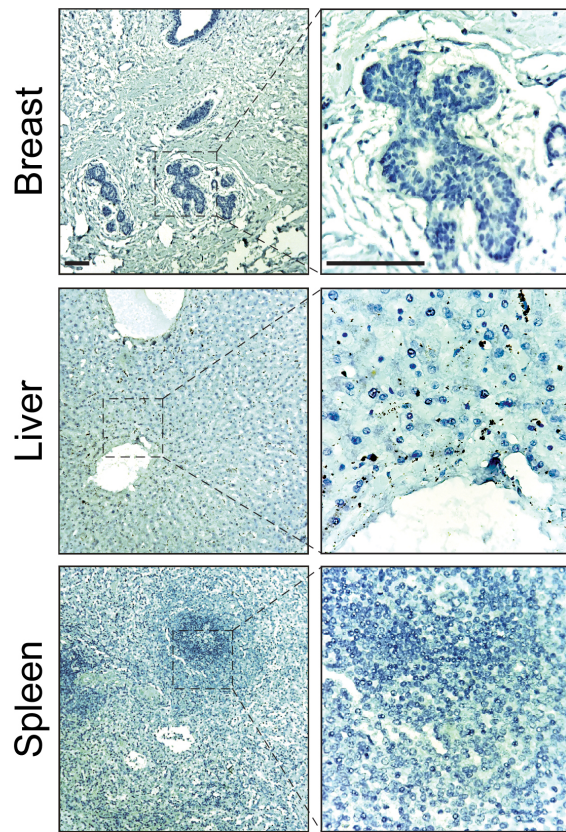
**Supplementary Figure 4. Specificity of the rabbit polyclonal antibody to mNdnf**

A rabbit antibody was generated using full-length of mouse Ndnf. HEK 293T cells were transfected to express Myc-tagged mouse Ndnf. Cell lysates were collected 48 hours after transfection. Tagged Ndnf was detected by Western blot using the antibody against Myc (left) and rabbit anti-Ndnf (right). Myc-tagged mouse Ndnf is ~75 kD.

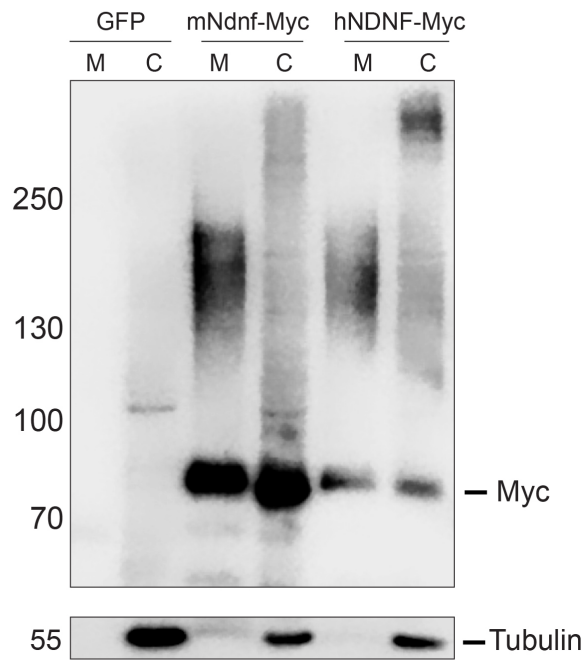


**Supplementary Figure 5. Negative control for RNAscope *in situ* hybridization**

Negative controls for panels C and D in Figure 2. RNAscope *in situ* hybridization of *NDNF/Ndnf* mRNA was detected by sense probes in the normal adult mouse (A) and human (B) lung. Cell nuclei are counterstained with Hematoxylin (Blue). Experiments were carried out in parallels with those shown in Figure 2. Scale bar, 100  $\mu$ m.

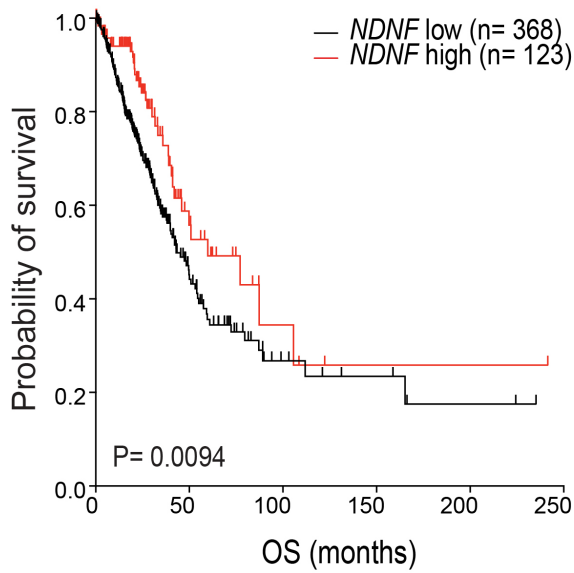


**Supplementary Figure 6. Lack of *NDNF* expression in the normal adult human breast, liver and spleen.** RNAscope *in situ* hybridization detection of *NDNF* mRNA (red) expression in the normal adult human breast, liver, and spleen. Cell nuclei are counterstained with Hematoxylin (Blue). *NDNF* mRNA analysis of human lung is shown in Fig. 2D. Scale bar, 100  $\mu$ m.



**Supplementary Figure 7. Mouse *Ndnf* and human *NDNF* encode secreted proteins.**

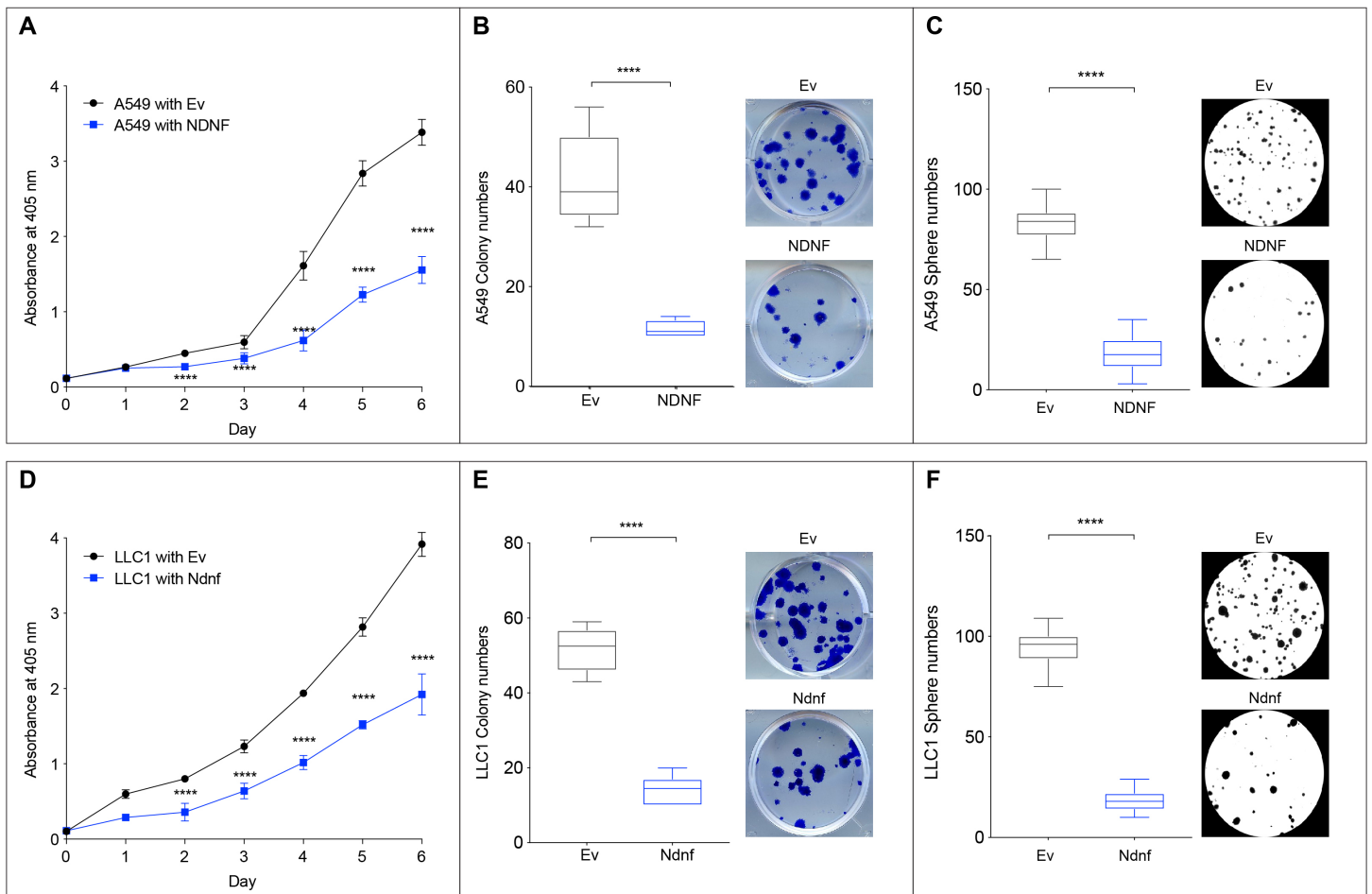
HEK 293T cells were transfected to express Myc-tagged mouse *Ndnf* or Myc-tagged human *NDNF*. Cell lysates (C) and the conditioned media (M) were collected 48 hours after transfection. The tagged versions of *Ndnf* and *NDNF* were detected by Western blot with an antibody against the Myc tag.



**Supplementary Figure 8. Higher *NDNF* expression is associated with better clinical outcome of lung adenocarcinoma patients**

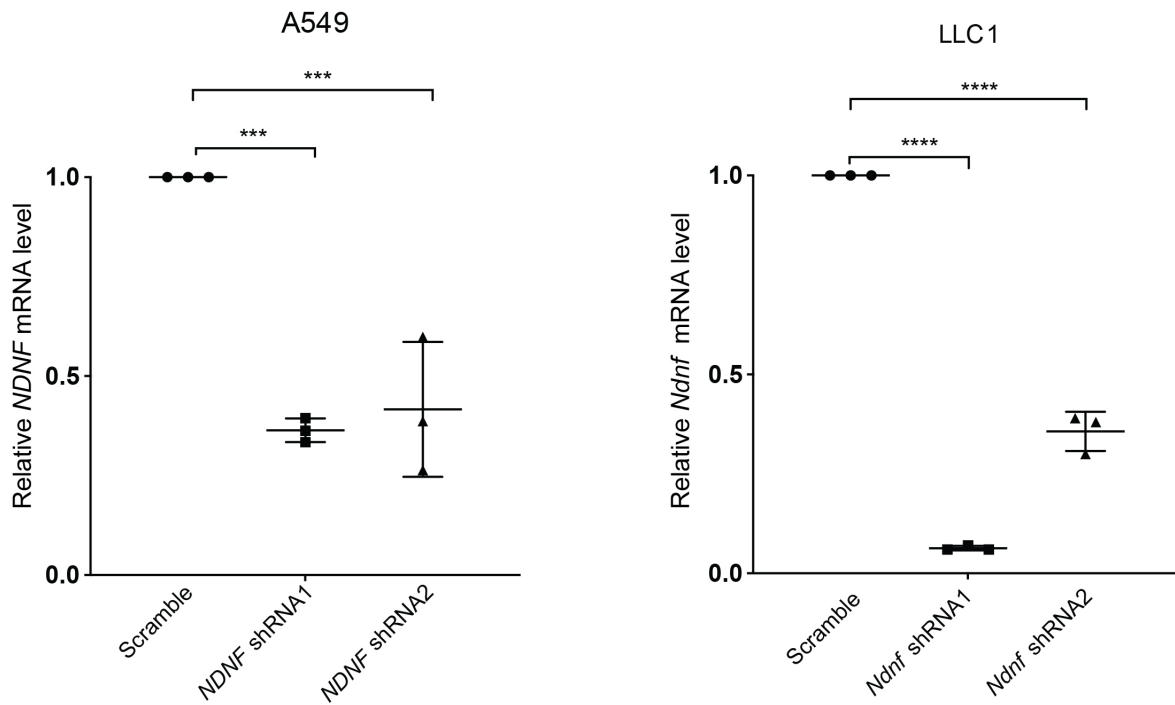
Kaplan-Meier curves showing the correlation between *NDNF* expression and overall survival (OS) of lung adenocarcinoma patients from the TCGA database ([Supplementary Table 4](#)). Lung adenocarcinoma patients were grouped according to the upper quartile expression of *NDNF*. The number of samples in the high/low *NDNF* groups and the log-rank p value are indicated on the graph.



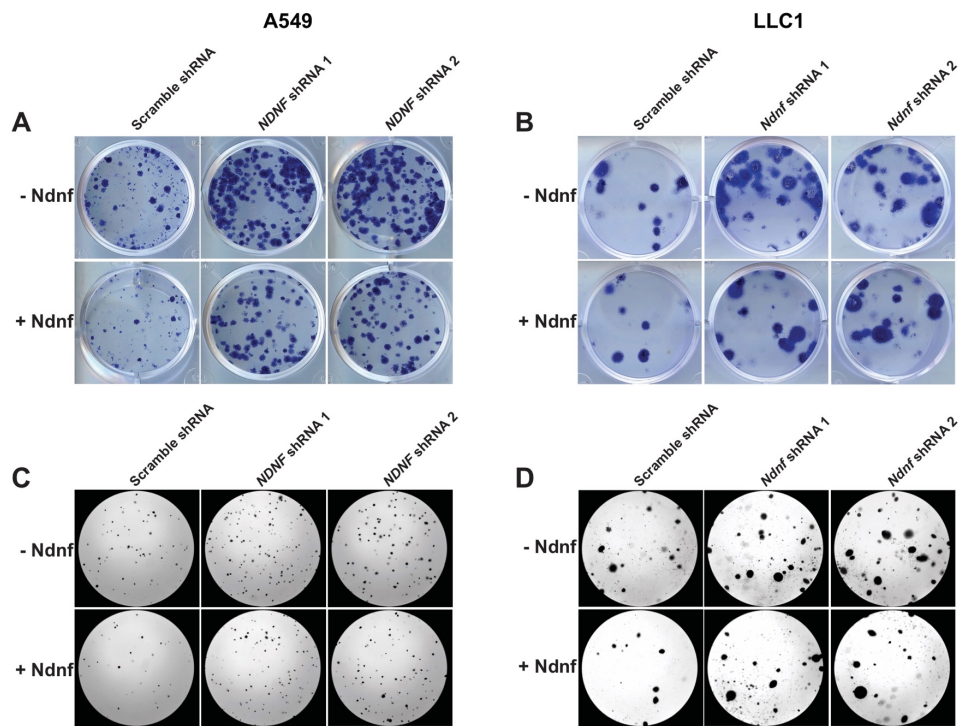


### Supplementary Figure 9. Tumor-suppressive properties of NDNF/Ndnf in human and mouse lung cancer cell lines

Effect of ectopic NDNF/Ndnf on the growth of human A549 (A-C) and mouse LLC1 (D-F) lung cancer cell lines. (A, D) Quantitative analysis of cell viability using the CCK8 assay of different cancer cells with or without overexpressed NDNF/Ndnf. Data are shown as mean  $\pm$  SD of  $n > 3$  replicates of a single experiment. Data are representative of  $n \geq 3$  experiments. (B, C, E, F) Quantitative analysis of cell growth using colony formation assay of cancer cells with or without overexpressed NDNF/Ndnf. Representative images from the colony formation assay are shown on the right side in each panel. Data are shown as box and whiskers plots of  $n \geq 6$  replicates from  $n \geq 3$  experiments. Box plots show 25th to 75th percentile; whiskers extend to the minimum and maximum values. The two-tailed Mann-Whitney U test was used for statistical analysis. \*\* $P < 0.01$ , \*\*\* $P < 0.001$ , and \*\*\*\* $P < 0.0001$ .

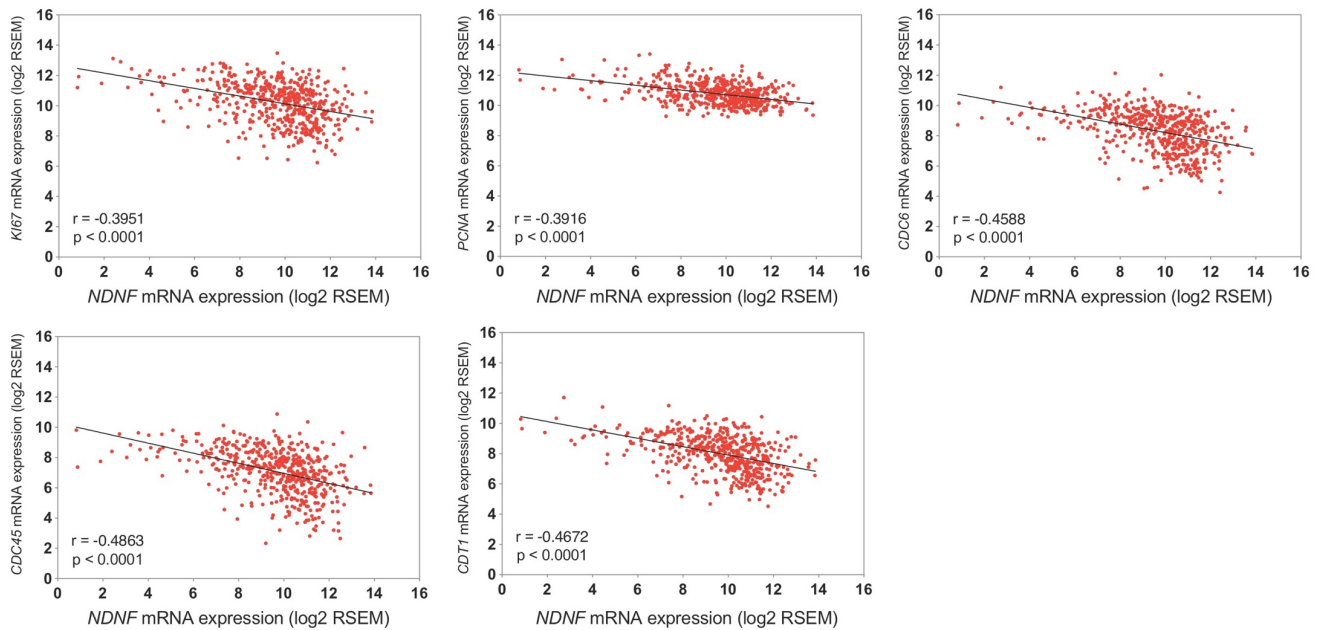


**Supplementary Figure 10. Knockdown efficiency of shRNA targeting human *NDNF* and mouse *Ndnf***  
 Knockdown efficiency of shRNAs targeting human *NDNF* in A549 cells and shRNAs targeting mouse *Ndnf* in LLC1 cells, compared with control scrambled shRNA, was determined by RT-qPCR analysis. Data are shown as mean  $\pm$  SD of n=3 replicates. Data are representative of n> 3 experiments. One-way ANOVA followed by Sidak's multiple comparison test was used for statistical analysis. \*\*\*P < 0.001, and \*\*\*\*P < 0.0001.



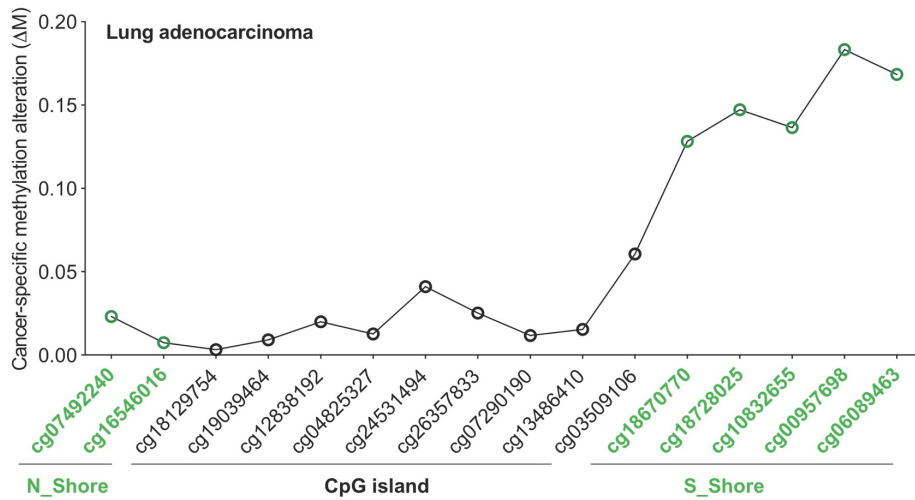
**Supplementary Figure 11. Effect of shRNA-based knockdown of *NDNF* or *Ndnf* on the growth of human or mouse lung cancer cells**

(A, B) Representative images from the colony formation assay with A549 and LLC1 cells. (C, D) Representative images from the soft agar formation assay with A549 and LLC1 cells. Quantitative analyses are shown in [Fig. 5](#).



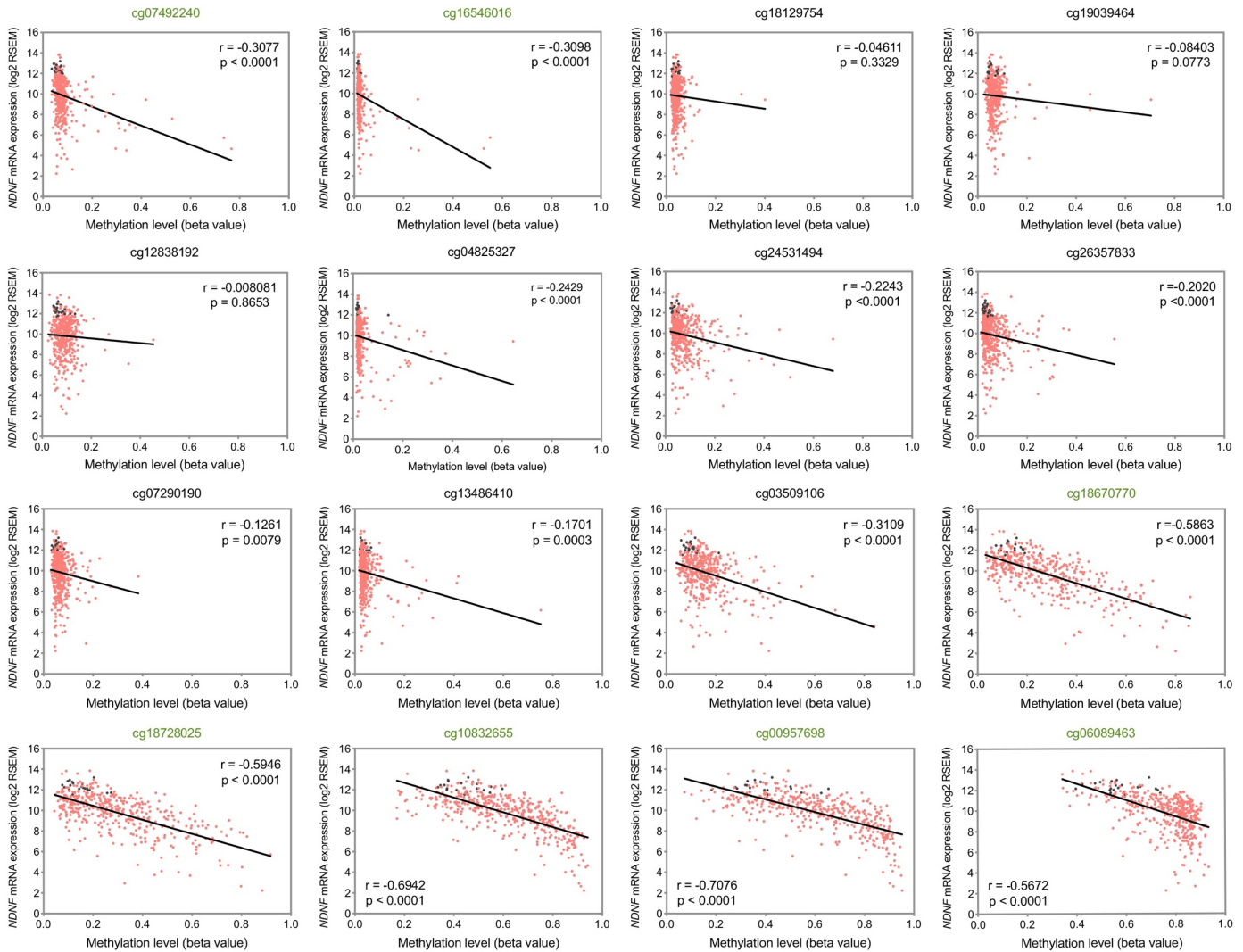
**Supplementary Figure 12. Negative correlations between *NDNF* expression and expression of proliferation-related genes in lung adenocarcinoma.**

Correlations between mRNA expression of *NDNF* and expression of genes encoding proliferation-related proteins (KI67, PCNA, CDC6, CDC45, and CDT1) in lung adenocarcinoma tissues samples from TCGA database. Spearman r and P values for each tissue are indicated in each panel.

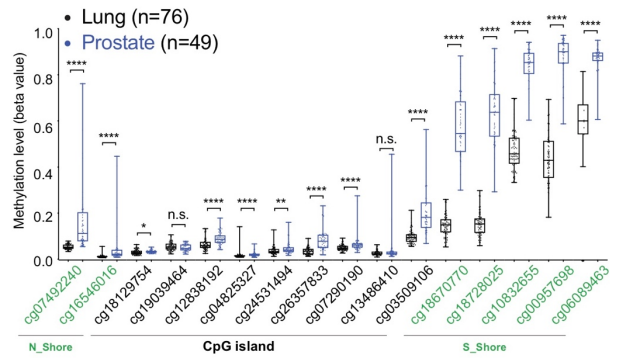
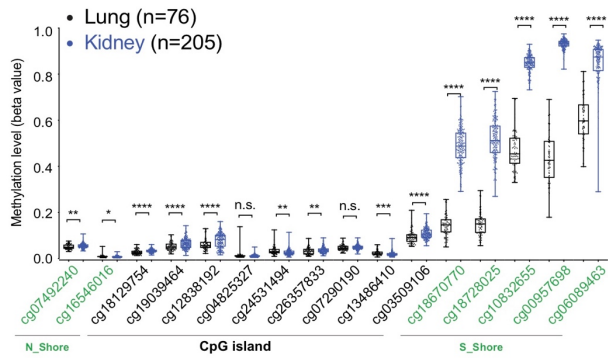
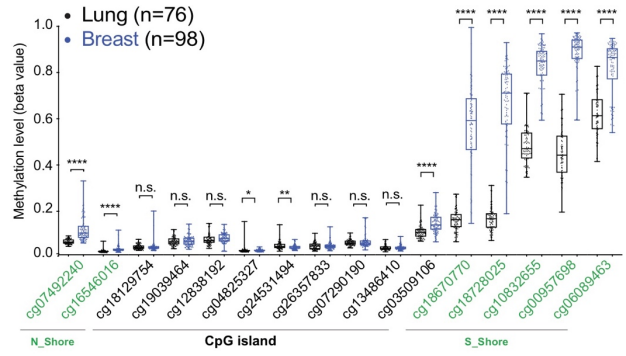
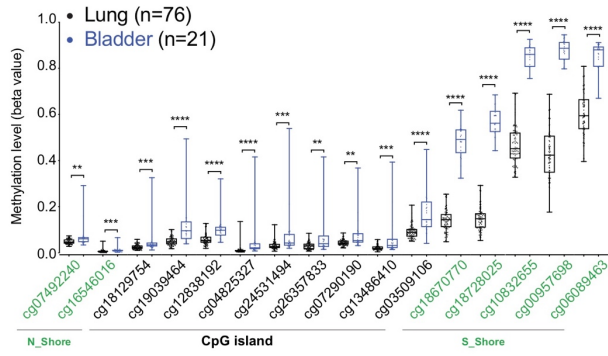


**Supplementary Figure 13. DNA methylation alterations in lung adenocarcinoma across 16 CpG sites in the *NDNF* promoter region**

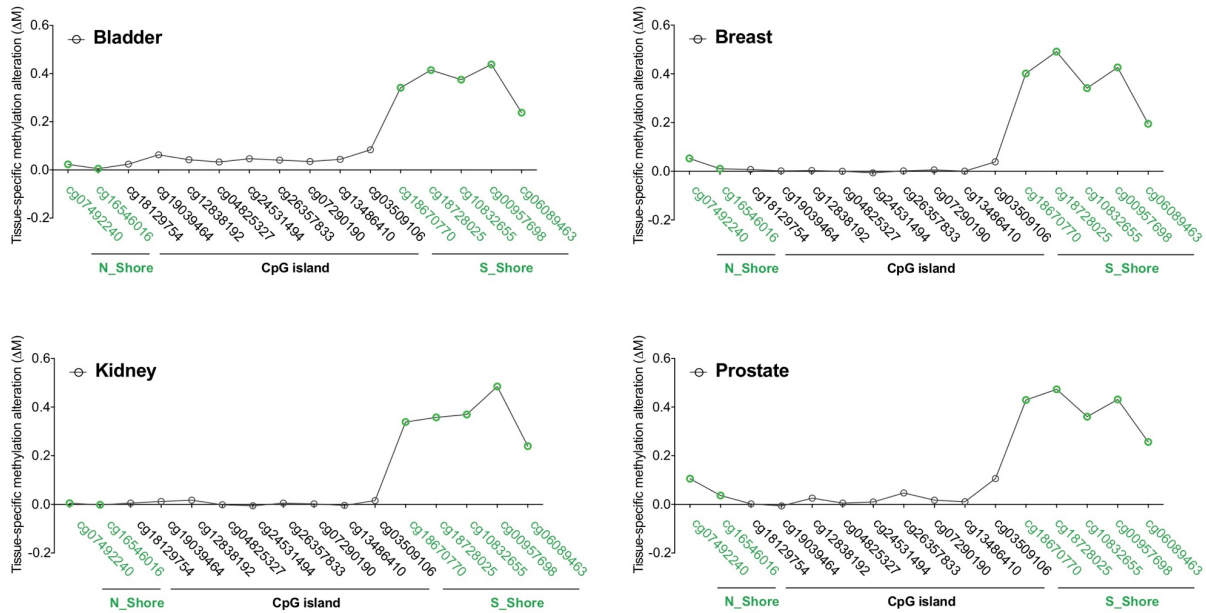
Cancer-specific methylation alterations ( $\Delta M$ ) were calculated for each of the 16 CpG sites in the *NDNF* promoter region. The  $\Delta M$  values are the difference in average DNA methylation between lung adenocarcinoma tissues and the average for normal lung from tissue adjacent to tumors (from averages in Fig. 7B). These values were used in Fig. 7F and Supplementary Fig. 18.



**Supplementary Figure 14. Correlation analysis of the relationship between *NDNF* expression and the DNA methylation at individual CpG sites in the *NDNF* promoter region in lung adenocarcinoma**  
 Scatter plots and correlation values between *NDNF* mRNA abundance and the average methylation level at each of the 16 CpG sites in the *NDNF* promoter region in tumor (n=422, red dots) and normal lung tissue adjacent to the tumor (n=21, black dots) from TCGA lung adenocarcinoma database. Spearman r and P values for each CpG sites are indicated in each panel.



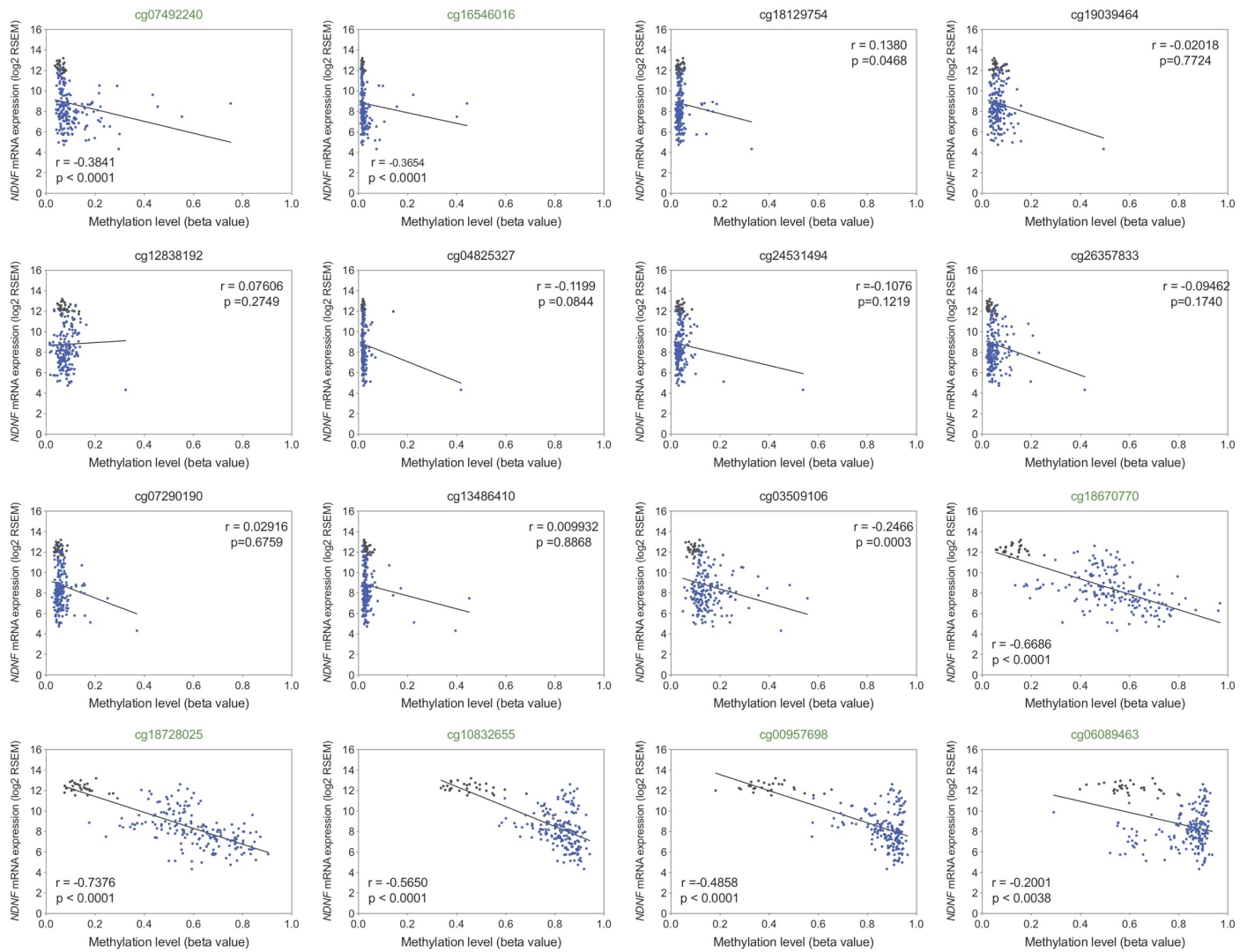
**Supplementary Figure 15. Differential methylation in the *NDNF* promoter region in different tissues**  
Methylation level at each of the 16 CpG sites in the *NDNF* promoter region in normal lung tissues (black) compared with other indicated normal tissues (blue). Methylation data for normal tissues are from tissue samples adjacent to tumors from the TCGA database. Box plots show 25th to 75th percentile whereas whiskers extend to the minimum and maximum values. The two-tailed Mann-Whitney U test was used for statistical analysis. n.s., not significant, \* $P < 0.05$ , \*\* $P < 0.01$ , \*\*\* $P < 0.001$ , and \*\*\*\* $P < 0.0001$ .



**Supplementary Figure 16. DNA methylation alterations in different tissues across 16 CpG sites in the *NDNF* promoter region**

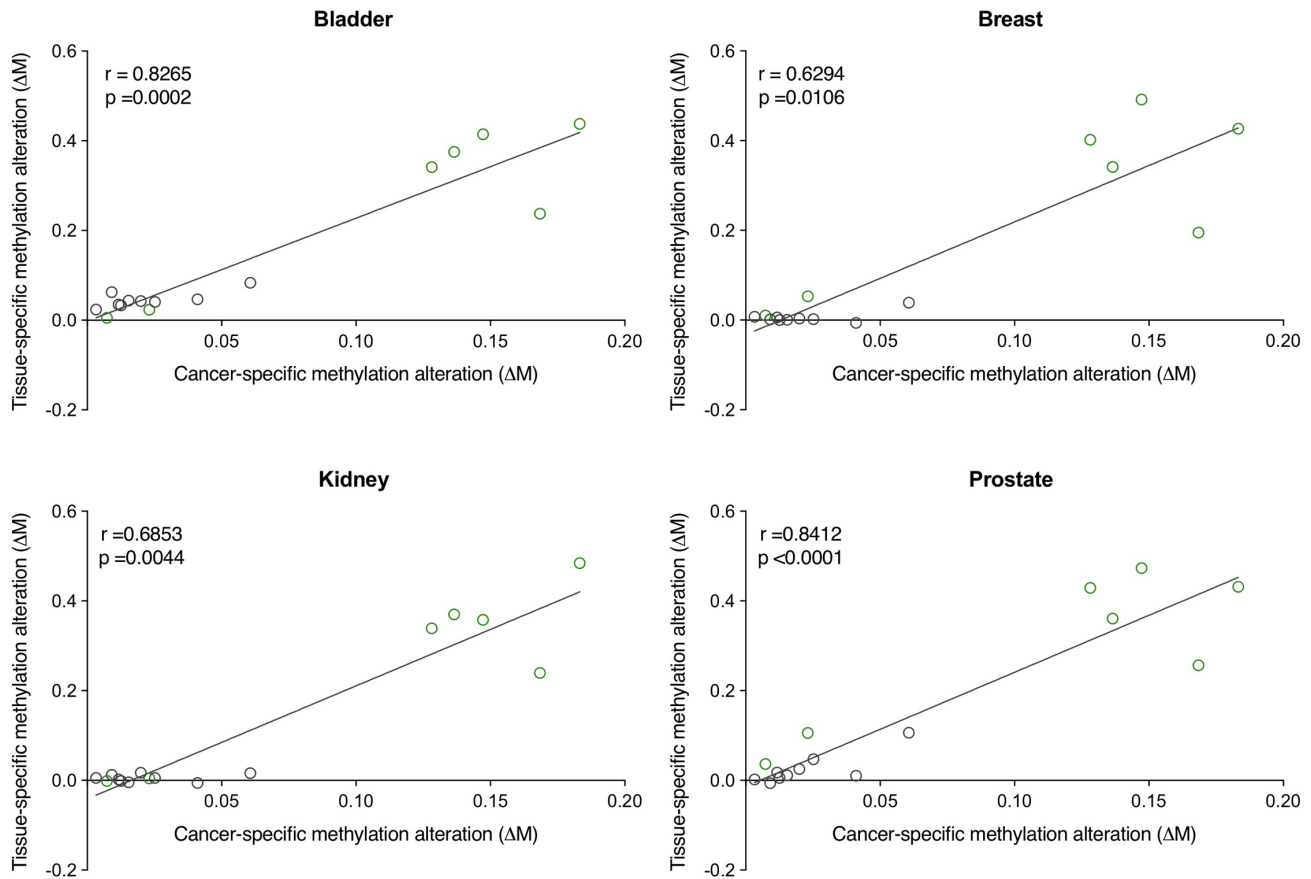
Tissue-specific differences in DNA methylation ( $\Delta M$ ) were calculated at each of the 16 CpG sites in the *NDNF* promoter region. The  $\Delta M$  values are the difference in the average methylation level in normal lung tissue and the average in the indicated normal tissue (from the averages in [Supplementary Fig. 15](#)). Methylation data for normal tissues are from tissue samples adjacent to tumors from the TCGA database. These values were used in [Supplementary Fig. 18](#).





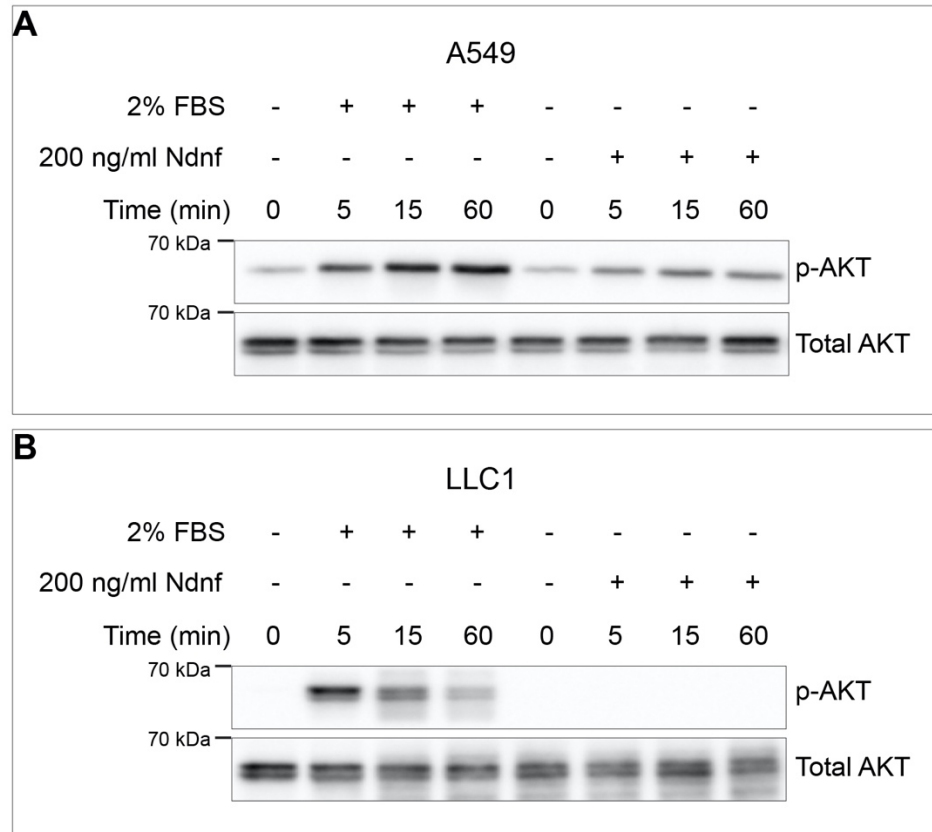
**Supplementary Figure 17. Correlation analysis of the relationships between *NDNF* expression and DNA methylation at individual CpG sites in the *NDNF* promoter region in different tissues**

Scatter plots and correlation values between *NDNF* transcript abundance and the average methylation level at each of the 16 CpG sites in the *NDNF* promoter region in samples from normal lung, bladder, breast, kidney, and prostate tissues adjacent to tumor from TCGA. Lung samples shown as black dots, all others as blue dots. Spearman r and P values are indicated.



**Supplementary Figure 18. Positive correlations between tissue-specific DNA methylation alterations and cancer-specific methylation alterations across the 16 CpG sites in the *NDNF* promoter region for 4 tissues.**

Scatter plot and correlation between alterations in tissue-specific DNA methylation and alterations in cancer-specific methylation at each of the 16 CpG sites in the *NDNF* promoter region. Each circle represents a CpG site: CpG island shores (green circles); CpG islands (black circles). Tissue-specific DNA methylation alterations were calculated as the difference in DNA methylation ( $\Delta M$ ) between the average methylation for each tissue (bladder, breast, kidney, or prostate) and lung (Supplementary Fig. 16); cancer-specific methylation alterations were calculated as the difference in DNA methylation between the average for lung adenocarcinoma tissues and the average for normal lung from tissue adjacent to tumors (from averages in Fig. 7B; Supplementary Fig. 13). Spearman r and P values are indicated.



**Supplementary Figure 19. Effect of Ndnf on AKT signaling in human and mouse lung cancer cell lines**  
 Phosphorylation levels of AKT in human A549 (A) and mouse LLC1 (B) lung cancer cells were determined by Western blot analysis. Briefly, confluent cultures of A549 or LLC1 cells were rendered quiescent after a 24-h incubation in serum-free DMEM media. Cultures were then washed and incubated with DMEM media containing serum (2%FBS, positive control) or Ndnf protein (200 ng/ml) for 5, 15 and 60 min at 37 °C with 5% CO<sub>2</sub>. Cell lysates were then collected in the presence of phosphatase inhibitor and fractionated by SDS-PAGE. Proteins were electrophorated onto polyvinylidene difluoride membranes and Western-blotted with either anti-phospho (Ser-473)-AKT antibody (p-AKT) or anti-AKT antibody (total AKT). Note: compared to 2% FBS, Ndnf protein has little or no effect on AKT signaling activity in tested lung cancer cell lines. Data are representative of n> 3 experiments.